

Original articles

Research article

<https://doi.org/10.17308/kcmf.2024.26/11808>

Synthesis and luminescent properties of PbS/SiO₂ core-shell quantum dots

I. G. Grevtseva✉, M. S. Smirnov, K. S. Chirkov, A. N. Latyshev, O. V. Ovchinnikov

Voronezh State University,
1 Universitetskaya pl., Voronezh 394018, Russian Federation

Abstract

The research focuses on the development of techniques for creating core-shell structures, based on colloidal PbS quantum dots (PbS QDs) and establishing the influence of the dielectric SiO₂ shell on the luminescent properties of PbS QDs. The objects of the study were PbS QDs with an average size of 3.0±0.5 nm, passivated with thioglycolic acid (TGA) and PbS/SiO₂ QDs, based on them with an average size of 6.0±0.5 nm. When we passivated the PbS QD interfaces with thioglycolic acid molecules, there were two luminescence peaks at 1100 and at 1260 nm. It was found that increasing the temperature of the colloidal mixture to 60 °C provides an increase in the intensity of the long-wave peak. An analysis of the luminescence excitation spectra of both bands and the Stokes shift showed that the band at 1100 nm is associated with the radiative annihilation of an exciton, while the band at 1260 nm is due to recombination at trap levels. The formation of PbS/SiO₂ QDs suppresses trap state luminescence, indicating the localization of luminescence centers predominantly at QD interfaces. The exciton luminescence at 1100 nm becomes more intensive.

Keywords: Lead sulfide quantum dots, Core-shell structures, SiO₂ shell, Luminescence spectra, Excitation spectra

Funding: The study was funded by the Russian Science Foundation, research project No. 22-72-00098.

Acknowledgements: The results of transmission electron microscopy using a Libra 120 microscope were obtained with the help of the equipment of the Centre for Collective Use of Voronezh State University.

For citation: Grevtseva I. G., Smirnov M. S., Chirkov K. S., Latyshev A. N., Ovchinnikov O. V. Synthesis and luminescent properties of PbS/SiO₂ core-shell quantum dots. *Condensed Matter and Interphases*. 2024;26(1): 45–54. <https://doi.org/10.17308/kcmf.2024.26/11808>

Для цитирования: Гревцева И. Г., Смирнов М. С., Чирков К. С., Латышев А. Н., Овчинников О. В. Синтез и спектрально-люминесцентные свойства квантовых точек ядро/оболочка PbS/SiO₂. *Конденсированные среды и межфазные границы*. 2024;26(1): 45–54. <https://doi.org/10.17308/kcmf.2024.26/11808>

✉ Irina G. Grevtseva, e-mail: grevtseva_ig@inbox.ru

© Grevtseva I. G., Smirnov M. S., Chirkov K. S., Latyshev A. N., Ovchinnikov O. V., 2024



1. Introduction

Scientific and practical interest in semiconductor colloidal quantum dots (QDs) is determined by a wide range of their potential applications. They are based on photoprocesses that provide size-dependent absorption and luminescent properties [1–16]. So, controlling the luminescent properties of colloidal QDs is a topical task of modern nanophotonics. There are studies demonstrating that it is possible to control the luminescent properties of QDs due to both the quantum-size effect and structural and impurity defects in the volume and at the interfaces of QDs [16–25]. Semiconductor colloidal PbS QDs are of significant interest in this field, since they exhibit luminescent properties in the visible and near-IR ranges [12–16, 26–30], which is due to the energy of the band gap of the PbS bulk crystal, which is 0.41 eV [26]. Accordingly, it is relevant to control the spectral composition and quantum yield of emission for PbS QDs due to the wide range of their potential applications. These include optoelectronic device technologies (detectors, emitters, nonlinear media for intensity and phase control, sensor systems, etc.), photocatalytic systems, as well as biomedical applications (luminescent markers), etc. [1–16].

Colloidal synthesis techniques involve QDs surface passivation with organic ligands. The chemical properties of the organic ligand, its concentration, and mechanism of interaction with the QD surface determine the presence/absence of surface states in QDs [17–25]. Despite the fact that numerous colloidal synthesis techniques have been proposed for PbS QDs, which provide highly dispersed QDs, there is still the problem of controlling the luminescent properties [24–30]. The available literature data concerning the size dependence of spectral-luminescent properties, value of the Stokes shift, and luminescence mechanism for PbS QDs are contradictory and ambiguous [24, 25, 29–34]. When the energy structure of exciton states changes due to the variations in the size of PbS QDs or their surface environment, new luminescence bands are often formed in the luminescence spectra due to optical transitions of charge carriers on the trap states [14, 16, 24, 25]. According to the atomistic calculations of the energy structure of QDs using

the density functional theory (DFT) [24, 35], the emitting trap states are formed at the synthesis stage of colloidal PbS QDs. They are caused by the presence of reduced or “undercharged” Pb atoms on the surface of QDs. In this case, the emitting trap states in PbS QDs are removed by changing the ligand, pH or polarity of the medium, which also leads to the loss of exciton luminescence intensity [24]. For most colloidal QD compositions, optical transitions involving trap states in QDs are controlled by forming a shell of wide-band gap semiconductors on the surface of QDs (core-shell structures) [17, 36–38]. The formation of core-shell structures, based on PbS QDs, in particular PbS/SiO₂ QDs, has been little studied [27, 39–41]. Whereas the formation of the SiO₂ shells on the QD interfaces contributes not only to the “curing” of the structural and impurity defects of QDs, involved in the formation of luminescent properties, but also allows controlling the monodispersity of QDs in the ensemble, increasing the colloidal QDs stability, and decreasing cytotoxicity [17, 27, 36–41]. Thus, controlling the luminescent properties of PbS QDs, including through the formation of core-shell structures on their basis, is an urgent task. Resolving this problem will provide an opportunity to create materials and devices for modern nanophotonics applications, based on PbS QDs.

The aim of the study was to form a SiO₂ shell on the interfaces of PbS QDs and to determine its influence on the luminescent properties of PbS QDs.

2. Experimental

2.1. Methods for the synthesis of colloidal PbS QDs and PbS/SiO₂ QDs

Samples of colloidal PbS QDs were obtained by aqueous synthesis, using thioglycolic acid (TGA) molecules as an organic passivator of the QD interface. The process was based on the methodology for the synthesis of colloidal QDs, previously implemented for silver and cadmium sulfide QDs [14–21]. This synthesis procedure consisted of mixing aqueous solutions of TGA and Pb(NO₃)₂ with a molar ratio of 2:1, respectively, followed by adjusting the pH to 10. Next, an aqueous Na₂S solution was added to the reaction mixture with a molar ratio of 0.2:1 to Pb(NO₃)₂.

At this stage of the synthesis, a sample was taken (PbS QD#1 sample). Then, the colloidal mixture was kept at 60 °C for 1 hour (PbS QD#2 sample); for 2 hours (PbS QD#3 sample).

PbS/SiO₂ core-shell QD structures were also formed by an aqueous synthesis technique. It is based on the use of (3-mercaptopropyl)trimethoxysilane (MPTMS) silica ligand as a coupling agent and sodium metasilicate (Na₂SiO₃) as a SiO₂ main layer precursor [17, 36, 38]. The concentration of the added MPTMS solution was calculated, based on the concentration and average size of PbS QDs in the ensemble. It was ~ 0.2 mM for all PbS QD samples. Next, an aqueous solution of Na₂SiO₃ (0.5 mM) was added to the colloidal mixture and kept at room temperature for 24 h (samples PbS/SiO₂ QD#1, PbS/SiO₂ QD#2, and PbS/SiO₂ QD#3).

To avoid oxidation of PbS QDs, nitrogen purging was carried out during the synthesis stage. Afterwards, the obtained samples of PbS and PbS/SiO₂ QDs were stored at 5 °C.

2.2. Experimental techniques

The sizes of PbS QDs and core-shell structures of PbS/SiO₂ QDs, based on them were determined by transmission electron spectroscopy (TEM) using a Libra 120 microscope (CarlZeiss, Germany) and a digital analysis of TEM images and X-ray diffraction.

Photoluminescence spectra of PbS and PbS/SiO₂ QD samples in the near infrared range were recorded using a PDF 10C/M image sensor (ThorlabsInc., USA) with a built-in amplifier and a diffraction monochromator with a 600 mm⁻¹ grating. A NDB7675 semiconductor laser diode (Nichia, Japan) with the wavelength of 462 nm was used as a source of luminescence excitation. The luminescence spectra were corrected for the spectral characteristics of the devices which was measured using a reference incandescent lamp with a known color temperature.

To record the luminescence excitation spectra of PbS and PbS/SiO₂ QD samples, we used another diffraction monochromator with a 1200 mm⁻¹ grating and 400 W incandescent lamp. It provided the excitation range from 500 to 1300 nm. The intensity of the excitation radiation in the sample region was controlled by an optical power meter Thorlabs PM100A with Thermal Power Sensor

Head S401C, sensitive in the range of 0.19–20 μm. The excitation radiation power was in the range of 100–400 mW.

The quantum yield of luminescence for PbS and PbS/SiO₂ QDs was determined by the relative method using the equation:

$$QY = QY_r \frac{I}{I_r} \frac{D_r}{D} \frac{n^2}{n_r^2}, \quad (1)$$

where QY_r is the quantum yield of the reference luminescence, I and I_r are the integral intensities in the luminescence band of the QD sample and reference, D and D_r are the optical densities at the excitation wavelength for the QD sample and reference (in the experiments, D and $D_r \sim 0.1$), n and n_r are the refractive indices of the solutions of the studied QD sample and reference, respectively. Distilled water ($n = 1.33$ at a wavelength of 650 nm at 293 K [42]) served as a solvent for PbS and PbS/SiO₂ QDs. A DMSO solution of indocyanine green (ICG) dye with $QY_k = 12\%$ in the region of 800 nm [43] ($n_r = 1.47$ at a wavelength of 650 nm at 293 K according to [44]) was used as a reference for the quantum yield of luminescence of PbS and PbS/SiO₂ QDs in the near IR range.

3. Results and discussion

3.1. Structural data of the obtained PbS and PbS/SiO₂ QD samples

TEM images of all synthesized samples of PbS QDs showed that our synthesis procedure resulted in the formation of individual QDs with close average sizes in the range of 3.0±0.5 nm and dispersion within 25% (Fig. 1). X-ray diffraction data of all obtained samples of colloidal PbS QDs showed broadened reflections, which is due to the quantum size effect (Fig. 1). The observed peaks are correlated with the diffraction of atomic planes (111), (200), (220), (311), (222), (400), (311), and (420), indicating the formation of PbS nanocrystals in a cubic crystal lattice ($Fm\bar{3}m$) [45].

The formation of PbS/SiO₂ QDs leads to an increase in the average size of PbS QDs to 5.5–6.0 nm (Fig. 1), which is probably due to the presence of a SiO₂ layer with a thickness of about 1.3–1.5 nm on the surface of QDs. In some cases, agglomerates of PbS/SiO₂ QDs were formed (Fig. 1).

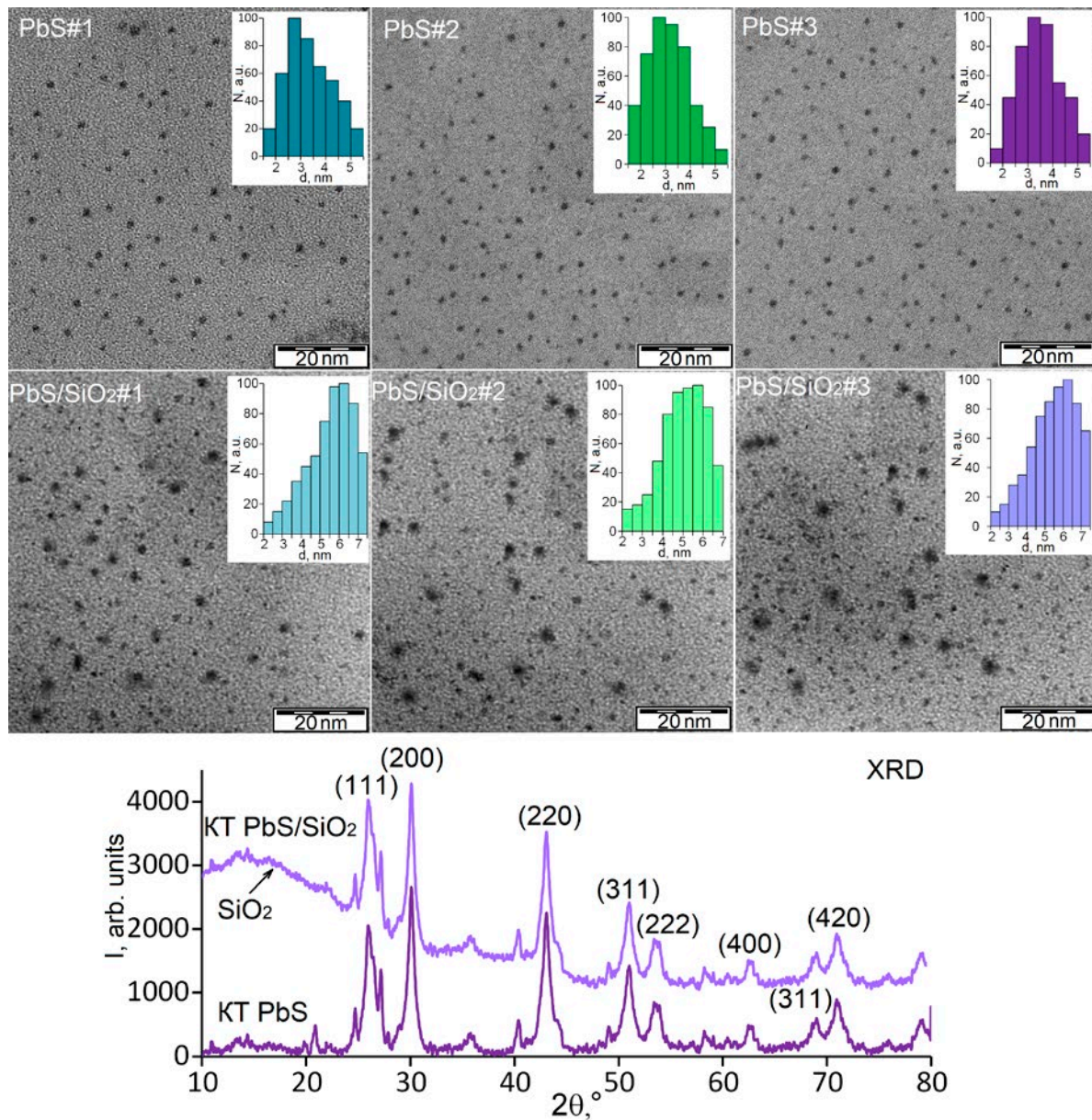


Fig. 1. TEM images and size distribution histograms of ensembles of PbS QDs and PbS/SiO₂ QDs. Diffractograms of PbS QDs and PbS/SiO₂ QDs

Also, during the formation of PbS/SiO₂ QDs, the diffraction pattern showed an additional diffuse band in the 2θ angle range from 15 to 40°. These changes in the diffraction were interpreted as the contribution of amorphous SiO₂ phase [46]. They were observed during the formation of the SiO₂ shell on the surface of QDs of other compositions [47, 48].

3.2. Spectral-luminescent properties of PbS QDs

UV-Vis absorption spectra of all PbS QD samples do not have an exciton structure, and

noticeable absorption begins in the wavelength range below 1000 nm (1.24 eV). Thus, the absorption edge of PbS QDs appears to be shifted toward shorter wavelengths compared to the absorption edge of PbS (3025 nm or 0.41 eV) [26]. It is a manifestation of quantum confinement effect. The structureless absorption edge characteristic of the studied samples may be due to a high concentration of defects [49, 50], as well as to a noticeable size dispersion of PbS QDs [51].

The luminescent properties of all obtained PbS QD samples turned out to be fundamentally different (Fig. 2).

The luminescence spectrum of the initial PbS QD#1 sample had a single band with a peak around 1100 nm (Fig. 2, curve 1). The luminescence band was not elementary, there was a specific feature in the long-wave part of the spectrum in the range of 1200–1280 nm. Keeping the samples of colloidal PbS QDs at 60 °C (PbS QD#2) for 1 hour resulted in the appearance of the second band in the luminescence spectrum in the region of 1260 nm (Fig. 2, curve 2). Subsequent of PbS QD samples at 60 °C for 2 hours (PbS QD#3) resulted in almost complete disappearance of the luminescence band at 1100 nm. In the luminescence spectrum, only one band at 1280 nm remained (Fig. 2, curve 3). The full width at half maximum (FWHM) of the luminescence band of PbS QDs for all studied samples was about 0.20–0.25 eV. Since the optical absorption spectra for all PbS QD samples do not have an exciton structure, we considered the luminescence excitation spectra (Fig. 2) to establish the luminescence mechanisms. As opposed to the absorption spectra that are determined by the absorption of each nanocrystal in the sample, only the QDs emitting at the recording wavelengths participate in the formation of the excitation spectra. This allowed achieving selectivity by the wavelength in the luminescence excitation spectra through a change in the recording wavelength [15, 16].

In the luminescence excitation spectra of all PbS QD samples, there is a specific feature with a peak at 980 nm in the short-wave band (1100 nm) (Fig. 2, curves 1', 2', and 3'). The position and shape of this peak suggest that it is associated with a probable exciton transition in the optical absorption spectrum. In this case, the Stokes shift of the luminescence peak at 1100 nm relative to the exciton absorption peak was 0.125 eV. On the contrary, no exciton structure was found in the excitation spectrum of the long-wave luminescence band with a peak at 1280 nm (Fig. 2, curves 1'', 2'', and 3''). The excitation band edge was located in the region of 980 nm, while the Stokes shift value increased up to 0.33 eV. The obtained data are

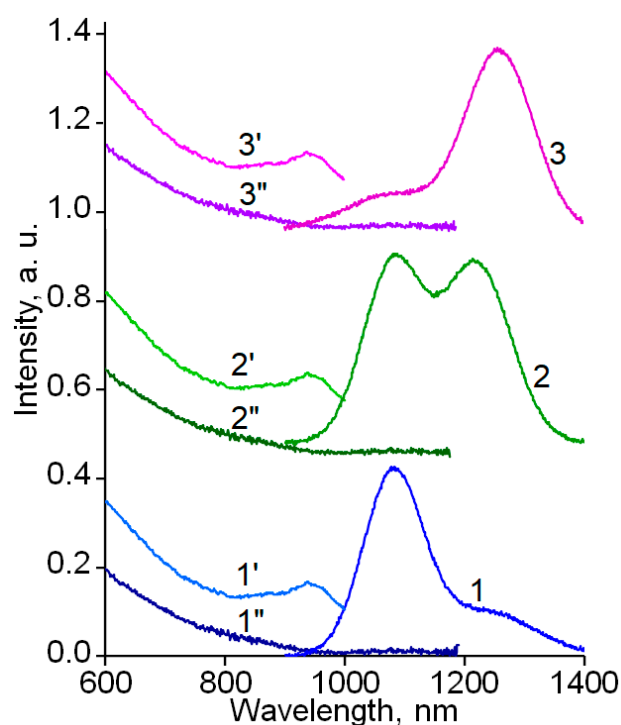


Fig. 2. Luminescence spectra of PbS QD#1 (1), PbS QD#2 (2), and PbS QD#3 (3). Luminescence excitation spectra in the region of 1100 nm (PbS QD#1 (1'), PbS QD#2 (2'), PbS QD#3 (3')) and 1260 nm (PbS QD#1 (1''), PbS QD#2 (2''), PbS QD#3 (3''))

in agreement with the data, obtained by the authors earlier [15, 16]. In study [16], based on experimental data on the temperature dependence of luminescence properties and luminescence excitation spectra of PbS QDs, a scheme defining IR luminescence was proposed. According to this scheme, the luminescence band at 1100 nm is due to the radiative annihilation of an exciton, and the long-wavelength band at 1260 nm is due to the recombination of free charge carriers on structural and impurity defects.

Thus, within the framework of a unified approach to the synthesis of PbS QDs, we obtained QD samples of close size but with different luminescent properties. According to the experimental data, the luminescence of PbS QD#1 is mainly due to exciton luminescence, PbS QD#2 is characterized by the simultaneous presence of both exciton and trap state luminescence bands in the spectrum, and the luminescence of PbS QD#3 is mainly due to trap state luminescence.

3.3. Spectral-luminescent properties of PbS/SiO₂ QDs

The main manifestations of core-shell PbS QDs formation were observed in the luminescence properties (Fig. 3).

The formation of PbS/SiO₂ QD#1 resulted in a shift of the exciton luminescence band from 1100 to 1080 nm, while the FWHM of the luminescence band decreased from 0.20 to 0.12 eV, and the quantum yield of luminescence increased from 2.5 to 4.5% (Fig. 3a, curves 1, 2). In the case of PbS QD#2 sample, upon the formation of the SiO₂ shell, the long-wave luminescence band in the region of 1260 nm, which was due to trap state luminescence, disappeared. At the same time, the luminescence band in the region of 1100 nm shifted to 1030 nm (Fig. 3b, curves 1, 2), its FWHM decreased from 0.25 to 0.13 eV, and the quantum yield increased from 1 to 3%. In the case of PbS QD#3, the formation of the shell resulted in the appearance of an intense luminescence band in the region of 1080 nm, while the band at 1260 nm shifted to a shorter wavelength of 1210 nm (Fig. 3c, curves 1, 2). The FWHM of both luminescence peaks was estimated to be within the range of 0.1–0.2 eV. No exciton structure was found in the luminescence excitation spectrum with a peak at 1210 nm. The excitation band edge

is located in the region of 950 nm, and the value of the Stokes shift is 0.3 eV (Fig. 3c, curves 2, 3), which is similar to the data for the original samples of PbS QD#3 and indicates the trap state nature of luminescence in the region of 1210 nm. The shift of the trap state luminescence peak to the shorter wavelength can probably be explained by the influence of the SiO₂ shell on the energy states of the structural and impurity defects of PbS QD#3. The quantum yield of PbS QD#3 remained unchanged upon the formation of the SiO₂ shell and amounted to 1.5 %.

For all PbS/SiO₂ QD samples, we recorded excitation spectra of the short-wavelength luminescence band (1030–1100 nm) due to exciton luminescence. They demonstrated a shift in the peak of the ground exciton transition to 900 nm compared to the peak in the region of 980 nm for PbS QDs (Fig. 3a, b, c, curves 4, 5). For PbS QD#1, the Stokes shift increased from 0.13 to 0.22 eV, for PbS QD#2 – from 0.13 to 0.17 eV, and for PbS QD#3 – from 0.13 to 0.22 eV. The observed regularities probably result from the change in the size distribution of PbS QDs in the ensemble during the formation of the SiO₂ shell [15]. Estimates of the average size of PbS QDs in the framework of the hyperbolic zone model [52] showed that the shift of the ground

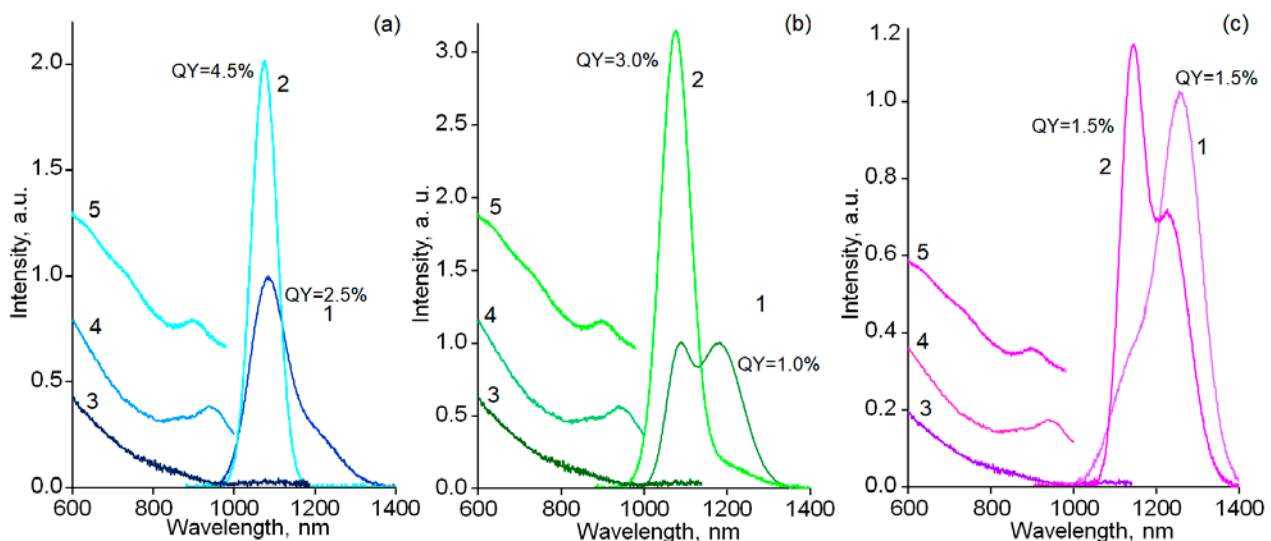


Fig. 3. Luminescence spectra of PbS QD#1 (1) and PbS/SiO₂ QD#1 (2) – a; PbS QD#2 (1) and PbS/SiO₂ QD#2 (2) – b; PbS QD#3 (1) и PbS/SiO₂ QD#3 (2) – c. Luminescence excitation spectra in the region of 1260 nm for PbS/SiO₂ QD#1 (3) – a; PbS/SiO₂ QD#2 (3) – b; PbS/SiO₂ QD#3 (3) – c. Luminescence excitation spectra in the region of 1100 nm for PbS QD#1 (4) – a; PbS QD#2 (4) – b; PbS QD#3 (4) – c. Luminescence excitation spectra in the region of 1080 nm for PbS/SiO₂ QD#1 (5) – a; PbS/SiO₂ QD#2 (5) – b; PbS/SiO₂ QD#3 (5) – c

exciton transition peak in the excitation spectra from 980 to 900 nm (0.1 eV) is due to a decrease in the diameter of PbS QDs within 0.4 nm. It is not possible to compare the obtained theoretical estimates of the QDs size change during the formation of core-shell structures with the TEM experimental data, since the TEM image of PbS/SiO₂ QDs is complicated by the presence of a contrast phase associated with the formation of the SiO₂ layer on the QD surface. The increase in the Stokes shift value as a result of the formation of the core-shell structure can also indicate an increase in the energy of the Coulomb and exchange interaction between the electron and hole in the exciton due to the enhancement of the quantum confinement of charge carriers [15].

Thus, the complete disappearance of the long-wavelength luminescence band at 1260 nm for PbS/SiO₂ QD#1 and PbS/SiO₂ QD#2, and its partial disappearance for PbS/SiO₂ QD#3 indicates the suppression of trap state luminescence in PbS QDs as a result of the formation of the SiO₂ shell. This suggests the interface nature of the luminescence centers.

4. Conclusions

The study presented the principles of controlling the IR luminescence of colloidal PbS QDs. The technique of colloidal synthesis of PbS QDs, passivated with thioglycolic acid molecules that we used in this work makes it possible to obtain PbS QDs with an average size of 3.0±0.5 nm, predominantly with luminescence in the region of 1100 nm. Keeping colloidal solutions of PbS QDs at 60 °C has no significant effect on the average size of QDs in the ensemble, but leads to the appearance of a long-wavelength luminescence band at 1260 nm. Analysis of the luminescence excitation spectra of both bands and the Stokes shift showed that the band at 1100 nm is associated with the radiative annihilation of an exciton, while the band at 1260 nm is due to recombination at trap state levels. Thus, radiative recombination centers are formed at the interfaces of PbS QDs under the effect of temperature.

The formation of a SiO₂ shell on the interfaces of PbS QDs with the exciton luminescence at 1100 nm leads to the shift of the luminescence band towards the short-wave region by 20 nm and

a twofold increase in the luminescence quantum yield. The shift of luminescence to shorter waves is presumably associated with a decrease in the average size of PbS QDs in the ensemble upon the formation of core-shell structures. In the case of PbS QDs characterized by trap-state luminescence at 1260 nm, the formation of the SiO₂ shell results in partial or complete quenching of trap-state luminescence with a simultaneous increase in the quantum yield of exciton luminescence in the range of 1030-1100 nm. Thus, PbS/SiO₂ QDs ensure the suppression of trap state luminescence in PbS QDs, which in turn indicates the interface nature of the luminescence centers.

Contribution of the authors

Grevtseva I. G. – Conceptualization, Methodology, Investigation, Original Draft Preparation & Editing. Smirnov M. S. – Research Concept, Researching, Original Draft Preparation, Review & Editing. Chirkov K. S. – Investigation, Software. Latyshev A. N. – Result Discussion, Review & Editing. Ovchinnikov O. V. – Conceptualization, Methodology, Writing the Text, Final Conclusions.

Conflict of interests

The authors declare that they have no known competing financial interests or personal relationships that could have influenced the work reported in this paper.

References

1. Hafiz S. B., Scimeca M., Sahu A., Ko D.-K. Colloidal quantum dots for thermal infrared sensing and imaging. *Nano Convergence*. 2019;6(7). <https://doi.org/10.1186/s40580-019-0178-1>
2. Sergeev A. A., Pavlov D. V., Kuchmizhak A. A., ... Rogach A. L. Tailoring spontaneous infrared emission of HgTe quantum dots with laser-printed plasmonic arrays. *Light: Science and Applications*. 2020;9(16). <https://doi.org/10.1038/s41377-020-0247-6>
3. Reineck P., Gibson B. C. Near-infrared fluorescent nanomaterials for bioimaging and sensing. *Advanced Optical Materials*. 2017;5: 1600446. <https://doi.org/10.1002/adom.201600446>
4. Gu Yi.-P., Cui R., Zhang Z.-L., Xie Z.-X., Pang D.-W. Ultrasmall near-infrared Ag₂Se quantum dots with tunable fluorescence for in vivo imaging. *Journal of the American Chemical Society*. 2012;134(1): 79–82. <https://doi.org/10.1021/ja2089553>
5. Xu S., Cui J., Wang L. Recent developments of low-toxicity NIR II quantum dots for sensing and

- bioimaging. *TrAC Trends in Analytical Chemistry*. 2016;80: 149–155. <https://doi.org/10.1016/j.trac.2015.07.017>
6. Zaini M. S., Liew J. Y. Ch., Ahmad S. A. A., Mohamad A. R., Kamarudin M. A. Quantum confinement effect and photoenhancement of photoluminescence of PbS and PbS/MnS quantum dots. *Applied Sciences*. 2020;10(18): 6282. <https://doi.org/10.3390/app10186282>
7. Tan L., Wan A., Zhao T., Huang R., Li H. Aqueous synthesis of multidentate-polymer-capping Ag₂Se quantum dots with bright photoluminescence tunable in a second near-infrared biological window. *ACS Applied Materials and Interfaces*. 2014;6(9): 6217–6222. <https://doi.org/10.1021/am5015088>
8. Keuleyan S., Lhuillier E., Guyot-Sionnest P. Synthesis of colloidal HgTe quantum dots for narrow Mid-IR emission and detection. *Journal of the American Chemical Society*. 2011;133(41): 16422–16424. <https://doi.org/10.1021/ja2079509>
9. Yu Y., Zhang K., Sun S. One-pot aqueous synthesis of near infrared emitting PbS quantum dots. *Applied Surface Science*. 2012;258(18): 7181–7187. <https://doi.org/10.1016/j.apsusc.2012.04.031>
10. Qian H., Dong C., Peng J., Qiu X., Xu Y., Ren J. High-quality and water-soluble near-infrared photoluminescent CdHgTe/CdS quantum dots prepared by adjusting size and composition. *The Journal of Physical Chemistry C*. 2007;111(45): 16852–16857. <https://doi.org/10.1021/jp074961c>
11. Capoen B., Martucci A., Turrell S., Bouazaoui M. Effects of the sol-gel solution host on the chemical and optical properties of PbS quantum dots. *Journal of Molecular Structure*. 2003;651-653: 467–473. [https://doi.org/10.1016/S0022-2860\(02\)00667-1](https://doi.org/10.1016/S0022-2860(02)00667-1)
12. Yin Q., Zhang W., Zhou Y., Wang R., Zhao Z., Liu C. High efficiency luminescence from PbS quantum dots embedded glasses for near-infrared light emitting diodes. *Journal of Luminescence*. 2022;250: 119065. <https://doi.org/10.1016/j.jlumin.2022.119065>
13. Srivastava R. R., Mishra H., Singh V. K., Vikram K., Srivastava R. K., Srivastava S. K., Srivastava A. pH dependent luminescence switching of tin disulfide quantum dots. *Journal of Luminescence*. 2019;213: 401–408. <https://doi.org/10.1016/j.jlumin.2019.05.024>
14. Zvyagin A. I., Chevychelova T. A., Chirkov K. S., Smirnov M. S., Ovchinnikov O. V. Size dependence of nonlinear optical properties of PbS QDs, passivated with thioglycolic acid. *Optik*. 2023;272: 170276. <https://doi.org/10.1016/j.ijleo.2022.170276>
15. Grevtseva I., Chevychelova T., Ovchinnikov O., ... Chirkov K. Size effect features and mechanism of luminescence of colloidal PbS quantum dots, passivated with thioglycolic acid. *Optical and Quantum Electronics*. 2023;55(5): 433. <https://doi.org/10.1007/s11082-023-04658-3>
16. Grevtseva I. G., Ovchinnikov O. V., Smirnov M. S., Chirkov K. S. Trap state and exciton luminescence of colloidal PbS quantum dots coated with thioglycolic acid molecules. *Condensed Matter and Interphases*. 25(2), 182–189. <https://doi.org/10.17308/kcmf.2023.25/11099>
17. Grevtseva I. G., Ovchinnikov O. V., Smirnov M. S., ... Vozgorkova. Photostability of luminescence of Ag₂S quantum dots and Ag₂S/SiO₂ core/shell structure. *Optics and Spectroscopy*. 2022;130(12): 1634–1644. <https://doi.org/10.21883/os.2022.12.54100.4106-22>
18. Smirnov M. S., Ovchinnikov O. V., Grevtseva I. G., Zvyagin A. I., Perepelitsa A. S., Ganeev R. A. Photoinduced degradation of the optical properties of colloidal Ag₂S and CdS quantum dots passivated by thioglycolic acid. *Optics and Spectroscopy*. 2018;124(5): 681–686. <https://doi.org/10.1134/S0030400X18050211>
19. Ovchinnikov O. V., Grevtseva I. G., Smirnov M. S., ... Matsukovich A. S. Effect of thioglycolic acid molecules on luminescence properties of Ag₂S quantum dots. *Optical and Quantum Electronics*. 2020;52(4): 198. <https://doi.org/10.1007/s11082-020-02314-8>
20. Ovchinnikov O. V., Grevtseva I. G., Smirnov M. S., Kondratenko T. S. Reverse photodegradation of infrared luminescence of colloidal Ag₂S quantum dots. *Journal of Luminescence*. 2019;207: 626–632. <https://doi.org/10.1016/j.jlumin.2018.12.019>
21. Kondratenko T., Ovchinnikov O., Grevtseva I., ... Tatianina E. Thioglycolic acid FTIR spectra on Ag₂S quantum dots interfaces. *Materials*. 2020;13(4): 909. <https://doi.org/10.3390/ma13040909>
22. Kloepfer J. A., Bradforth S. E., Nadeau J. L. Photophysical properties of biologically compatible CdSe quantum dot structures. *The Journal of Physical Chemistry B*. 2005;109(20): 9996–10003. <https://doi.org/10.1021/jp044581g>
23. Krivenkov V. A., Samokhvalov P. S., Linkov P. A., ... Nabiev I. Surface ligands affect photoinduced modulation of the quantum dots optical performance. *SPIE Proceedings*. 2014;9126: 91263. <https://doi.org/10.1117/12.2057828>
24. Hwang G. W., Kim D., Cordero J. M., ... Bawendi M. G. Identifying and eliminating emissive sub-bandgap states in thin films of PbS nanocrystals. *Advanced Materials*. 2015;27: 4481–4486. <https://doi.org/10.1002/adma.201501156>
25. Nelson C. A., Zhu X.-Y. Reversible surface electronic traps in PbS quantum dot solids induced by an order disorder phase transition in capping molecules. *Journal of the American Chemical Society*. 2012;134(18): 7592–7595. <https://doi.org/10.1021/ja3004649>

26. Scanlon W. W. Recent advances in the optical and electronic properties of PbS, PbSe, PbTe and their alloys. *Journal of Physics and Chemistry of Solids*. 1959;8: 423–428. [https://doi.org/10.1016/0022-3697\(59\)90379-8](https://doi.org/10.1016/0022-3697(59)90379-8)
27. Wang D., Qian J., Cai F., He S., Han S., Mu Y. 'Green'-synthesized near-infrared PbS quantum dots with silica-PEG dual-layer coating: ultrastable and biocompatible optical probes for in vivo animal imaging. *Nanotechnology*. 2012;23: 245701. <https://doi.org/10.1088/0957-4484/23/24/245701>
28. Zhang J., Jiang X. Confinement-dependent below-gap state in PbS quantum dot films probed by continuous-wave photoinduced absorption. *The Journal of Physical Chemistry B*. 2008;112:32: 9557–9560. <https://doi.org/10.1021/jp8047295>
29. Ushakova E. V., Litvin A. P., Parfenov P. S., ... Baranov A. V. Anomalous size-dependent decay of low-energy luminescence from PbS quantum dots in colloidal solution. *ACS Nano*. 2012;6(10): 8913–8921. <https://doi.org/10.1021/nn3029106>
30. Voznyy O., Levina L., Fan F., ... Sargent E. H. Origins of Stokes shift in PbS nanocrystals. *Nano Letters*. 2017;17(12): 7191–7195. <https://doi.org/10.1021/acs.nanolett.7b01843>
31. Lewis J. E., Jiang X. J. Unconventional gap state of trapped exciton in lead sulfide quantum dots. *Nanotechnology*. 2010;21: 455402. <https://doi.org/10.1088/0957-4484/21/45/455402>
32. Gaponenko M. S., Tolstik N. A., Lutich A. A., Onushchenko A. A., Yumashev K. V. Temperature-dependent photoluminescence Stokes shift in PbS quantum dots. *Physica E: Low-dimensional Systems and Nanostructures*. 2013;53: 63–65. <https://doi.org/10.1016/j.physe.2013.04.018>
33. Nakashima S., Hoshino A., Cai J., Mukai K. Thiol-stabilized PbS quantum dots with stable luminescence in the infrared spectral range. *Journal of Crystal Growth*. 2013;378: 542–545. <http://dx.doi.org/10.1016/j.jcrysgro.2012.11.024>
34. Moreels I., Lambert K., Smeets D., ... Hens Z. Size-dependent optical properties of colloidal PbS quantum dots. *ACS Nano*. 2009;3(10): 3023–3030. <https://doi.org/10.1021/nn900863a>
35. Giansante C., Infante I. Surface traps in colloidal quantum dots: A combined experimental and theoretical perspective. *The Journal of Physical Chemistry Letters*. 2017;8(20): 5209–5215 <https://doi.org/10.1021/acs.jpcclett.7b02193>
36. Ovchinnikov O. V., Perepelitsa A. S., Smirnov M. S., Aslanov S. V. Control the shallow trap states concentration during the formation of luminescent Ag₂S and Ag₂S/SiO₂ core/shell quantum dots. *Journal of Luminescence*. 2022;243: 118616. <https://doi.org/10.1016/j.jlumin.2021.118616>
37. Vasudevan D., Gaddam R. R., Trinchi A., Cole I. Core-shell quantum dots: Properties and applications. *Journal of Alloys and Compounds*. 2015;636(5): 395–404. <https://doi.org/10.1016/j.jallcom.2015.02.102>
38. Perepelitsa A. S., Ovchinnikov O. V., Smirnov M. S., ... Khokhlov V. Y. Structural and optical properties of Ag₂S/SiO₂ core/shell quantum dots. *Journal of Luminescence*. 2021;231: 117805. <https://doi.org/10.1016/j.jlumin.2020.117805>
39. Mukai K., Okumura I., Nishizaki Y., Yamashita S., Niwa K. Silica coating of PbS quantum dots and their position control using a nanohole on Si substrate. *Japanese Journal of Applied Physics*. 2018;57: 04FH01. <https://doi.org/10.7567/JJAP.57.04FH01>
40. Capoen B., Martucci A., Turrell S., Bouazaoui M. Effects of the sol-gel solution host on the chemical and optical properties of PbS quantum dots. *Journal of Molecular Structure*. 2023;651–653: 467–473. [https://doi.org/10.1016/S0022-2860\(02\)00667-1](https://doi.org/10.1016/S0022-2860(02)00667-1)
41. Dhlamini M. S., Terblans J. J., Ntwaeaborwa O. M., Joubert H. D., Swart H. C. Preparations and luminescent properties of PbS nanoparticle phosphors incorporated in a SiO₂ matrix. *Physica Status Solidi C*. 2008;5(2): 598–601. <https://doi.org/10.1002/pssc.200776808>
42. Kedenburg S., Vieweg M., Gissibl T., Giessen H. Linear refractive index and absorption measurements of nonlinear optical liquids in the visible and near-infrared spectral region. *Optical Materials Express*. 2012;2(11): 1588–1611. <https://doi.org/10.1364/ome.2.001588>
43. van Leeuwen F. W. B., Cornelissen B., Caobelli F., ... de Jong M. Generation of fluorescently labeled tracers – which features influence the translational potential? *EJNMMI Radiopharmacy and Chemistry*. 2017;2(15). <https://doi.org/10.1186/s41181-017-0034-8>
44. Kozma I. Z., Krok P., Riedle E. Direct measurement of the group-velocity mismatch and derivation of the refractive-index dispersion for a variety of solvents in the ultraviolet. *Journal of the Optical Society of America B*. 2005;22(7): 1479–1485. <https://doi.org/10.1364/JOSAB.22.001479>
45. Sadovnikov S. I., Kozhevnikova N. S., Rempel A. A., Pushin V. G. Microstructure of nanocrystalline PbS powders and films. *Inorganic Materials*. 2012;48(1): 21–27. <https://doi.org/10.1134/S002016851201013X>
46. Music S., Filipovic-Vincekovic N., Sekovanic L. Precipitation of amorphous SiO₂ particles and their properties. *Brazilian Journal of Chemical Engineering*. 2011;28(1): 89–94. <https://doi.org/10.1590/S0104-66322011000100011>
47. Zhong Q., Cao M., Hu H., ... Zhang Q., One-pot synthesis of highly stable CsPbBr₃@SiO₂ core-shell nanoparticles. *ACS Nano*. 2018;12(8): 8579–8587. <https://doi.org/10.1021/acs.nano.8b04209>

48. Li B., Fan H., Zhao Q., Wang C. Synthesis, characterization and cytotoxicity of novel multifunctional Fe₃O₄@SiO₂@GdVO₄:Dy³⁺ core-shell nanocomposite as a drug carrier. *Materials*. 2016;9(3): 149. <https://doi.org/10.3390/ma9030149>

49. Gilmore R. H., Liu Y., Shcherbakov-Wu W., ... Tisdale W. A. Epitaxial dimers and auger-assisted detrapping in PbS quantum dot solids. *Matter*. 2019;1(1): 250–265. <https://doi.org/10.1016/j.matt.2019.05.015>

50. Sadovnikov S. I., Rempel A. A. Nonstoichiometric distribution of sulfur atoms in lead sulfide structure. *Doklady Physical Chemistry*. 2009;428(1): 167–171. <https://doi.org/10.1134/S0012501609090024>

51. Ovchinnikov O. V., Smirnov M. S., Korolev N. V., Golovinski P. A., Vitukhnovsky A. G. The size dependence recombination luminescence of hydrophilic colloidal CdS quantum dots in gelatin. *Journal of Luminescence*. 2016;179: 413–419. <https://doi.org/10.1016/j.jlumin.2016.07.016>

52. Wang Y., Suna A., Mahler W., Kasowski R. PbS in polymers. From molecules to bulk solids. *The Journal of Chemical Physics*. 1987;87: 7315–7322. <https://doi.org/10.1063/1.453325>

Информация об авторах

Irina G. Grevtseva, Cand. Sci. (Phys.–Math.), Associate Professor, Department of Optics and Spectroscopy, Voronezh State University (Voronezh, Russian Federation).

<https://orcid.org/0000-0002-1964-1233>
grevtseva_ig@inbox.ru

Mikhail S. Smirnov, Dr. Sci. (Phys.–Math.), Professor, Department of Optics and Spectroscopy, Voronezh State University (Voronezh, Russian Federation).

<https://orcid.org/0000-0001-8765-0986>
smirnov_m_s@mail.ru

Kirill S. Chirkov, post-graduate student, Department of Optics and Spectroscopy, Voronezh State University (Voronezh, Russian Federation).

<https://orcid.org/0000-0003-0387-0733>
kirill200598@mail.ru

Anatoly N. Latyshev, Dr. Sci. (Phys.–Math.), Professor, Department of Optics and Spectroscopy, Voronezh State University (Voronezh, Russian Federation).

<https://orcid.org/0000-0002-7271-0795>
latyshev@phys.vsu.ru

Oleg V. Ovchinnikov, Dr. Sci. (Phys.–Math.), Full Professor, Dean of the Faculty of Physics, Head of the Department of Optics and Spectroscopy, Voronezh State University (Voronezh, Russian Federation).

<https://orcid.org/0000-0001-6032-9295>
ovchinnikov_o_v@rambler.ru

Received 22.03.2023; approved after reviewing 23.05.2023; accepted for publication 15.06.2023; published online 25.03.2024.

Translated by Anastasiia Ananeva